

Ack1 is a dopamine transporter endocytic brake that rescues a trafficking-dysregulated ADHD coding variant

Sijia Wu^a, Karl D. Bellve^b, Kevin E. Fogarty^b, and Haley E. Melikian^{a,1}

^aBrudnick Neuropsychiatric Research Institute, University of Massachusetts Medical School, Worcester, MA 01604; and ^bBiomedical Imaging Group, Program in Molecular Medicine, University of Massachusetts Medical School, Worcester, MA 01605

Edited by Leslie Lars Iversen, University of Oxford, Oxford, United Kingdom, and approved November 4, 2015 (received for review July 3, 2015)

The dopamine (DA) transporter (DAT) facilitates high-affinity presynaptic DA reuptake that temporally and spatially constrains DA neurotransmission. Aberrant DAT function is implicated in attention-deficit/hyperactivity disorder and autism spectrum disorder. DAT is a major psychostimulant target, and psychostimulant reward strictly requires binding to DAT. DAT function is acutely modulated by dynamic membrane trafficking at the presynaptic terminal and a PKC-sensitive negative endocytic mechanism, or “endocytic brake,” controls DAT plasma membrane stability. However, the molecular basis for the DAT endocytic brake is unknown, and it is unknown whether this braking mechanism is unique to DAT or common to monoamine transporters. Here, we report that the *cdc42*-activated, nonreceptor tyrosine kinase, Ack1, is a DAT endocytic brake that stabilizes DAT at the plasma membrane and is released in response to PKC activation. Pharmacologic and shRNA-mediated Ack1 silencing enhanced basal DAT internalization and blocked PKC-stimulated DAT internalization, but had no effects on SERT endocytosis. Both *cdc42* activation and PKC stimulation converge on Ack1 to control Ack1 activity and DAT endocytic capacity, and Ack1 inactivation is required for stimulated DAT internalization downstream of PKC activation. Moreover, constitutive Ack1 activation is sufficient to rescue the gain-of-function endocytic phenotype exhibited by the ADHD DAT coding variant, R615C. These findings reveal a unique endocytic control switch that is highly specific for DAT. Moreover, the ability to rescue the DAT(R615C) coding variant suggests that manipulating DAT trafficking mechanisms may be a potential therapeutic approach to correct DAT coding variants that exhibit trafficking dysregulation.

dopamine | ADHD | membrane trafficking | tyrosine kinase | reuptake

Dopamine (DA) is a modulatory neurotransmitter critical for locomotion and reward (1), and dopaminergic (DAergic) dysregulation is linked to multiple neuropsychiatric disorders, including Parkinson’s disease, schizophrenia, attention-deficit/hyperactivity disorder (ADHD), and autism spectrum disorder (ASD) (2, 3). Presynaptic recapture, facilitated by the high-affinity DA transporter (DAT), spatially and temporally restricts extracellular DA availability (4–6). Addictive psychostimulants that target DAT and its monoamine transporter homologs for 5HT (SERT) and NE (NET) are either competitive ligands, such as cocaine, or competitive substrates, such as amphetamine (7). Although these drugs interact with DAT, SERT, and NET with equimolar affinity, their binding to DAT is requisite for reward (8, 9). Transporter inhibitors with differential DAT, SERT, and NET specificity are widely used to treat neuropsychiatric disorders (10, 11). However, their therapeutic efficacy differs significantly among patients, consistent with the model that monoamines may differentially contribute to the pathogenesis of these disorders (10, 12). Thus, regulatory mechanisms specific to DAT, SERT, or NET may provide a novel route to develop transporter-specific therapeutics.

DAT plasma membrane expression is requisite for efficacious extracellular DA removal and to replenish presynaptic DA stores (13). Indeed, DAT allelic and coding variants have been identified in a variety of neuropsychiatric disorders, including ADHD, ASD,

infantile Parkinsonism, and bipolar disorder (14–20), underscoring that even subtle DAT functional changes exert impactful consequences on DAergic neurotransmission. DAT is acutely regulated by membrane trafficking, and either protein kinase C (PKC) activation or AMPH exposure rapidly deplete DAT surface expression (5, 7, 21, 22). Intriguingly, a DAT coding variant, R615C, identified in an ADHD proband, exhibits profound membrane instability due to highly accelerated basal endocytosis (16), suggesting that dysregulated DAT membrane trafficking may contribute to the etiology of DA-related disorders.

Studies from our laboratory (23) and others (24) indicate that a unique negative regulatory mechanism, or “endocytic brake,” stabilizes DAT surface expression. PKC activation releases the endocytic brake, accelerates DAT internalization, and thereby reduces DAT surface levels and function. The cellular basis of this negative regulatory mechanism are completely undefined. Moreover, it is unknown whether the endocytic brake exists in DAergic terminals and whether it is specific to DAT.

Activated by *cdc42* kinase 1 (Ack1) is a nonreceptor tyrosine kinase that is a major *cdc42* effector activated via EGF, PDGF, and m3 muscarinic receptor stimulation (25, 26). Ack1 binds directly to clathrin heavy chain (27, 28) and is enriched in presynaptic terminals (29). Importantly, Ack1 is inactivated by PKC (26), and a recent study demonstrated that Ack1 overexpression suppresses endocytosis (30). Given these attributes, we asked whether

Significance

The dopamine (DA) transporter (DAT) stringently controls brain DA levels. Several addictive psychostimulants, antidepressants, and attention-deficit/hyperactivity disorder (ADHD) therapeutics inhibit DAT function, and multiple DAT mutants have been reported in ADHD, autism spectrum disorder, and infantile Parkinsonism. Given that aberrant DAT function underlies many pathological conditions, it is critical to understand intrinsic regulatory mechanisms that modulate DAT function. DAT availability at the cell surface is dynamically modulated, but the mechanisms controlling this process are not well understood. In the current study, we identified the penultimate mechanism that controls DAT stability at the cell surface. Moreover, by genetically manipulating this mechanism, we successfully rescued an ADHD-associated DAT mutant with intrinsic membrane instability. Thus, targeting DAT regulatory mechanisms may be a viable approach for treating dysregulated DAT.

Author contributions: S.W., K.D.B., K.E.F., and H.E.M. designed research; S.W. performed research; K.D.B. and K.E.F. contributed new reagents/analytic tools; S.W. and H.E.M. analyzed data; S.W. and H.E.M. wrote the paper; and K.D.B. provided technical support for TIRF microscopy experiments.

The authors declare no conflict of interest.

This article is a PNAS Direct Submission.

¹To whom correspondence should be addressed. Email: Haley.Melikian@umassmed.edu.

This article contains supporting information online at www.pnas.org/lookup/suppl/doi:10.1073/pnas.1512957112/-DCSupplemental.

Ack1 activity is the penultimate step that engages the DAT endocytic brake.

Results

Ack1 Negatively Regulates DAT, but Not SERT Endocytosis. Ack1 and its active, autophosphorylated form, pY284-Ack1 (pAck1) (25, 31), were readily detected in both the DAergic cell line SK-N-MC and mouse striatum (Fig. S1A and B). PKC activation significantly decreased pAck1 in both SK-N-MC cells ($46.5 \pm 3.0\%$ control levels; Fig. S1A) and mouse striatum ($78.3 \pm 5.2\%$ control levels; Fig. S1B). Likewise, the highly specific Ack1 inhibitor AIM-100 (32) dose-dependently decreased pAck1 in SK-N-MC cells (Fig. S1C) and dramatically decreased mouse striatal pAck1 to $13.2 \pm 2.2\%$ control levels (Fig. S1D). Thus, Ack1 is expressed in DAergic cell lines and striatum, and either PKC activation or AIM-100 inactivates Ack1 in both these model systems.

We predicted that if Ack1 imposes the DAT endocytic brake, then Ack1 inactivation would release the brake and decrease both DAT function and surface expression. Indeed, AIM-100 significantly decreased [3 H]DA uptake in SK-N-MC cells ($IC_{50} = 50.2 \pm 9.9 \mu\text{M}$) and striatal slices (Fig. 1A and B) and significantly reduced DAT surface levels to $72.5 \pm 6.4\%$ control levels in mouse striatum (Fig. 1C). DAT surface loss in response to AIM-100 was due to a significant increase in the DAT internalization rate, to

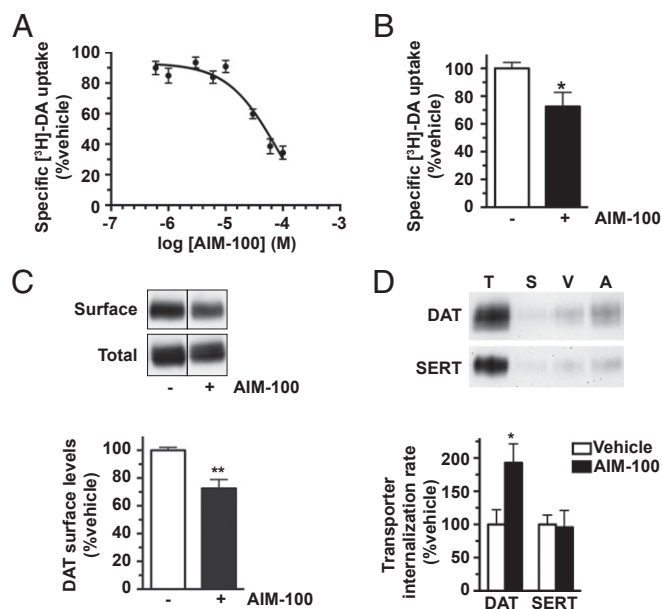


Fig. 1. Ack1 activity stabilizes DAT at the plasma membrane. (A) [3 H]DA uptake. DAT SK-N-MC cells were treated with the indicated AIM-100 concentrations for 30 min at 37 °C, and [3 H]DA uptake was measured as described in *SI Methods*. Data are expressed as percent specific DA uptake \pm SEM ($n = 12$). (B) Ex vivo slice uptake. Striatal slices were treated $\pm 20 \mu\text{M}$ AIM-100, 60 min, 37 °C and [3 H]DA uptake was assessed as described in *SI Methods*. * $P < 0.05$, Student's t test, $n = 6$ hemislices obtained from two independent mice. (C) Ex vivo slice biotinylation. Striatal slices were treated $\pm 20 \mu\text{M}$ AIM-100 for 30 min at 37 °C, and surface proteins were isolated by biotinylation as described in *SI Methods*. (C, Upper) Representative immunoblots. (C, Lower) Average DAT surface levels expressed as percent vehicle-treated levels \pm SEM. ** $P < 0.01$, Student's t test, $n = 3$. (D) Internalization assays. DAT and SERT internalization rates were measured in SK-N-MC cells $\pm 20 \mu\text{M}$ AIM-100 as described in *SI Methods*. (D, Upper) Representative immunoblots showing the total DAT and SERT surface pools at $t = 0$ (T), strip control (S), and internalized protein during either vehicle (V) or AIM-100 (A) treatments. (D, Lower) Average internalization rates expressed as percent vehicle-treated \pm SEM. * $P < 0.02$, Student's t test; $n = 5$ (DAT); $n = 3$ (SERT).

$192.9 \pm 28.6\%$ control levels (Fig. 1D), demonstrating that Ack1 negatively regulates DAT endocytosis. AIM-100 effects were specific to DAT and had no effect on the SERT endocytic rate measured in SERT-SK-N-MC cells (Fig. 1D; $P = 0.89$). Interestingly, high AIM-100 concentrations ($>20 \mu\text{M}$) inhibited DAT function to a much larger degree than what could be attributed to membrane trafficking. DAT loss of function was not due to transmembrane Na^+ gradient disruption, as AIM-100 had no effect on Na^+ -dependent alanine uptake (Fig. S2A). To our surprise, AIM-100 also dose-dependently inhibited SERT function (Fig. S2B), despite exerting no effect on SERT trafficking (Fig. 1D). We noted that AIM-100 bears DAT and SERT pharmacophore properties similar to piperazine derivatives, such as GBR12909 (Fig. S2C). We therefore hypothesized that, in addition to its known function as a high-affinity Ack1 inhibitor, AIM-100 may also be a low-affinity, competitive DAT and SERT inhibitor. Whole cell binding studies revealed that AIM-100 competitively inhibited DAT and SERT binding to [3 H]WIN 35428 and [3 H]imipramine, respectively (Fig. S2D), supporting the premise that AIM-100 is a DAT and SERT inhibitor. However, GBR12909 had no effect on pAck1 levels (Fig. S2E), indicating that DAT ligand binding does not globally inactivate Ack1. Moreover, a 10-fold lower AIM-100 concentration that efficaciously decreased p284-Ack1 levels ($2 \mu\text{M}$; Fig. S1C), also significantly increased DAT internalization rates (Fig. S2F). Thus, distinct endocytic mechanisms regulate DAT and SERT, and Ack1 activity is required to impose the DAT endocytic brake. Moreover, AIM-100 is, coincidentally, a low-affinity, competitive DAT and SERT inhibitor.

Constitutive and Regulated DAT Endocytosis Are Differentially Dependent on Clathrin. Ack1 is recruited to clathrin-coated pits via clathrin heavy chain interactions (27, 28). Thus, we hypothesized that clathrin is required to release the Ack1-imposed brake. To test clathrin-dependence, we acutely inhibited clathrin with pitstop2 and measured DAT internalization \pm AIM-100 and \pm PMA. Pitstop2 pretreatment significantly attenuated both AIM-100- and PKC-stimulated DAT internalization, but had no effect on basal DAT endocytosis (Fig. 2A and B), suggesting that stimulated DAT endocytosis is clathrin-dependent, whereas constitutive DAT endocytosis is clathrin-independent. We further used total internal resonance fluorescence microscopy (TIRFM) to examine clathrin and surface DAT under basal conditions, compared with transferrin receptor (TfR), a protein known to undergo robust clathrin-mediated endocytosis. Alexa 594-Tf colocalized markedly with eGFP-clathrin across the plasma membrane, and distinct Tf/clathrin puncta moved away from the TIRF field during imaging, consistent with clathrin-mediated endocytosis (Fig. 2C). In contrast, TagRFP-T-DAT was diffusely distributed across the plasma membrane and was enriched in cellular microspikes, with little apparent clathrin colocalization (Fig. 2C). Taken together with the pitstop2 data, these data support that constitutive DAT endocytosis is clathrin-independent, whereas stimulated DAT endocytosis requires clathrin.

Cdc42 Negatively Regulates DAT, but Not SERT, Endocytosis. Ack1 is a major cdc42 effector, suggesting that cdc42 may contribute to the DAT endocytic brake, upstream of Ack1. To test this possibility, we measured DAT surface levels in DAT SK-N-MC cells and striatal DAergic terminals following acute treatment with two structurally distinct cdc42 inhibitors, casin and pir11. Both casin and pir11 significantly reduced DAT surface levels in SK-N-MC cells (Fig. 3A and B), and casin significantly decreased surface DAT in mouse striatum (Fig. 3C). DAT surface loss in response to cdc42 inhibition was due to profound DAT endocytic acceleration ($238.0 \pm 15.5\%$ control levels, Fig. 3D). In contrast, pir11 did not significantly affect SERT internalization (Fig. S3A). We further tested whether PKC and cdc42 impact DAT surface stability in independent or convergent manners. Pretreatment \pm casin

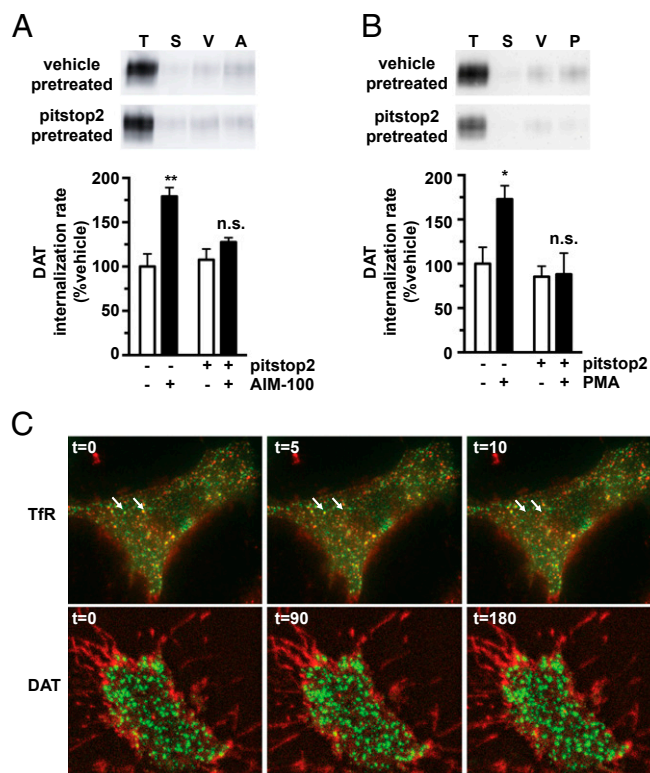


Fig. 2. Stimulated DAT endocytosis is clathrin-dependent, whereas constitutive DAT endocytosis is clathrin-independent. (A and B) DAT internalization assay. DAT SK-N-MC cells were pretreated $\pm 25 \mu\text{M}$ pitstop2 for 10 min at 37°C and rapidly chilled, and DAT internalization rates were measured as described in *SI Methods* $\pm 20 \mu\text{M}$ AIM-100 (A) or $\pm 1 \mu\text{M}$ PMA (B). (A and B, Upper) Representative immunoblots showing total surface DAT at $t = 0$ (T), strip control (S), and internalized DAT during vehicle (V), AIM-100 (A), or PMA (P) treatments. (A and B, Lower) Average DAT internalization rates expressed as percent vehicle-treated \pm SEM. Asterisks indicate a significant difference from vehicle. $*P < 0.03$; $***P < 0.005$, one-way ANOVA with Bonferroni's multiple comparison test; $n = 7$ (A); $n = 4-6$ (B). (C) TIRF microscopy. Time-lapse TIRF images were captured as described in *SI Methods*. (C, Upper) SK-N-MC cells stably expressing eGFP-clathrin labeled with Tf-Alexa594. White arrows indicate Tf/clathrin colocalized puncta that move away from the TIRF field during image capture. (C, Lower) SK-N-MC cells stably cotransfected with TagRFP-T-DAT and eGFP-clathrin.

(Fig. 3A) or \pm pir11 (Fig. 3B) significantly attenuated PKC-stimulated DAT endocytosis. Moreover, pir11 and PMA coapplication had no additive effect on DAT internalization (Fig. 3D). Taken together, these results demonstrate that *cdc42* activity is required to impose the DAT endocytic brake, likely via the same pathway as PKC and potentially upstream of Ack1. Moreover, these results further support that distinct endocytic mechanisms govern DAT and SERT surface stability.

Ack1 Inactivation Is Required to Release the DAT Endocytic Brake, Downstream of PKC or *cdc42*. We next used two efficacious hAck1-targeted shRNAs, 10 and 12 (Fig. S4A), to test whether Ack1 is required to (i) engage the DAT endocytic brake and (ii) stimulate DAT endocytosis by PKC activation or *cdc42* inhibition. The most efficacious hAck1 shRNA, 10, significantly increased basal DAT endocytosis to $138.7 \pm 12.3\%$ control levels (Fig. 4B), consistent with Ack1's requisite role as the DAT endocytic brake. Moreover, Ack1 depletion with either shRNA 10 or 12 significantly attenuated stimulated DAT endocytosis, either via PKC stimulation (Fig. 4C) or *cdc42* inhibition (Fig. 4D). In sum, these results support that Ack1 is required to engage the DAT endocytic brake.

Although perturbing Ack1 enhanced DAT endocytosis, we next asked whether there is a direct causal link between Ack1 inactivation and either *cdc42* inhibition or PKC activation to release the DAT endocytic brake. To test this, we coexpressed DAT with either wild-type, constitutively active (S445P), or kinase dead (K158A) Ack1 isoforms (33) (see Fig. S4B for Ack1 mutant overexpression profiles). We predicted that if Ack1 inactivation were required to release the DAT endocytic brake, then S445P-Ack1 would block accelerated DAT internalization in response to either PKC activation or *cdc42* inhibition. Wild-type Ack1 overexpression had no effect on basal or accelerated DAT endocytosis in response to PKC activation or *cdc42* inhibition (Fig. 5 B-D). In

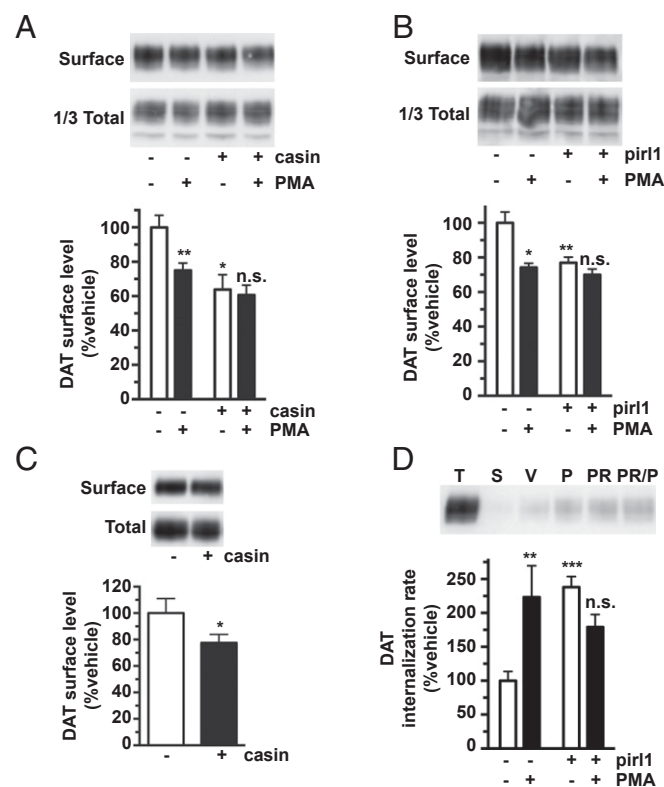


Fig. 3. *Cdc42* stabilizes DAT surface expression. (A and B) Cell surface biotinylation. DAT SK-N-MC cells were pretreated $\pm 10 \mu\text{M}$ casin (A) or $\pm 20 \mu\text{M}$ pir11 (B) for 30 min at 37°C , followed by treatment $\pm 1 \mu\text{M}$ PMA for 30 min at 37°C . Relative DAT surface levels were measured by biotinylation as described in *SI Methods*. Representative immunoblots are shown at the top of each panel. (A) Casin treatment. Average DAT surface levels expressed as percent vehicle levels \pm SEM. Asterisks indicate a significant difference from vehicle control. $*P < 0.05$; $**P < 0.01$, one-way ANOVA with Bonferroni's multiple comparison test; $n = 5-6$. (B) Pir11 treatment. Average DAT surface levels expressed as percent vehicle levels \pm SEM. Asterisks indicate a significant difference from vehicle control. $*P < 0.02$; $**P < 0.01$, one-way ANOVA with Bonferroni's multiple comparison test; $n = 3$. (C) Ex vivo striatal slice biotinylation. Mouse striatal slices were treated $\pm 10 \mu\text{M}$ casin for 30 min at 37°C , and relative DAT surface levels were measured by biotinylation as described in *SI Methods*. (C, Upper) Representative immunoblot. (C, Lower) Average DAT surface levels expressed as percent vehicle-treated \pm SEM. $*P < 0.05$, Student's *t* test; $n = 10$. (D) Internalization assay. DAT internalization rates were measured $\pm 1 \mu\text{M}$ PMA, $\pm 20 \mu\text{M}$ pir11, or with PMA/pir11 coapplication for 10 min at 37°C , as described in *SI Methods*. (D, Upper) Representative immunoblots showing total surface DAT at $t = 0$ (T), strip control (S), and internalized DAT during vehicle (V), PMA (P), or pir11 (PR) treatments. (D, Lower) Average DAT internalization rates expressed as percent vehicle rate \pm SEM. Asterisks indicate a significant difference from vehicle control. $**P < 0.01$; $***P < 0.005$, one-way ANOVA with Bonferroni's multiple comparison test; $n = 9-13$.

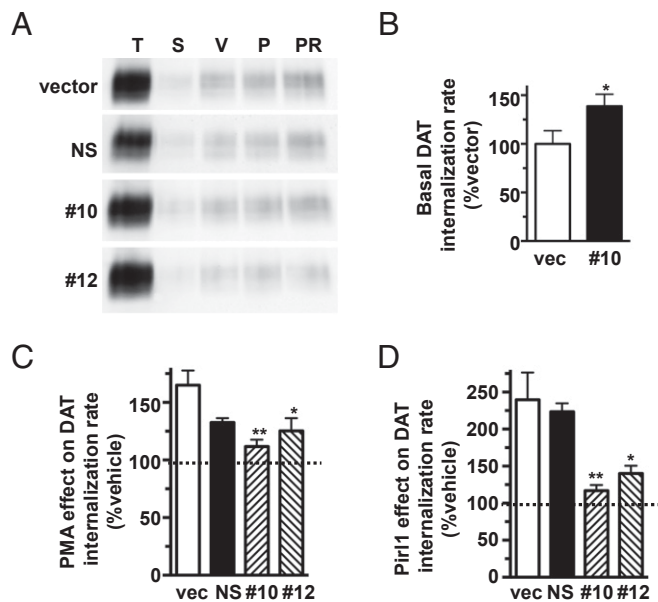


Fig. 4. shRNA-mediated Ack1 depletion increases basal DAT internalization and abolishes stimulated DAT endocytosis in response to PKC activation or cdc42 inhibition. (A–D) DAT internalization assays: DAT SK-N-MC cells were transduced with lentiviral particles expressing either pGIPZ vector (vec), non-silencing (NS), hAck1 10 (10), or hAck1 12 (12) shRNAs, and DAT internalization rates were measured $\pm 1 \mu\text{M}$ PMA (C) or $\pm 20 \mu\text{M}$ pirl1 (D) as described in *SI Methods*. (A) Representative immunoblots for each transduction condition showing total surface DAT at $t = 0$ (T), strip control (S), and internalized DAT during vehicle (V), PMA (P) or pirl1 (PR) treatments. (B) Basal DAT internalization rates expressed as percent vector-transduced rates \pm SEM. $*P < 0.04$, Student's *t* test; $n = 6$. (C) PKC-stimulated DAT internalization rates expressed as percent vehicle rate \pm SEM for each transduction condition. Asterisks indicate a significant difference from vector-transduced control. $*P < 0.03$; $**P < 0.01$, one-way ANOVA with Dunnett's multiple comparison test; $n = 4$ –7. (D) Pirl1-induced DAT internalization rates expressed as percent vehicle rate \pm SEM for each transduction condition. Asterisks indicate a significant difference from vector-transduced control, $*P < 0.02$; $**P < 0.01$, one-way ANOVA with Dunnett's multiple comparison test; $n = 4$ –7.

contrast, S445P-Ack1 significantly attenuated both PKC-stimulated (Fig. 5C) and pirl1-stimulated (Fig. 5D) DAT internalization. K158A-Ack1 had no significant effect either basal ($P = 0.30$) or pirl1-stimulated ($P = 0.30$) DAT internalization (Fig. 5B and D), but significantly inhibited PKC-stimulated DAT endocytosis ($100.1 \pm 5.2\%$ control level, Fig. 5C). Although the K158A mutant lacks kinase activity (34), it was unknown, a priori, whether this mutant would exert a dominant negative effect. Ack1 activation is required for targeting to clathrin-coated pits (30). Thus, it is not surprising the kinase dead mutant failed to exert a dominant effect on DAT internalization. Taken together, these results provide a causal link between upstream PKC or cdc42 stimuli and Ack1 inactivation as requisite steps in releasing the DAT endocytic brake.

Ack1 Activity Restores Normal Trafficking to a DAT Coding Variant Expressed in an ADHD Proband. A recent study reported that a DAT coding variant, R615C, identified in an ADHD proband, lacks endocytic braking, resulting in enhanced basal endocytosis and inability to undergo PKC- and AMPH-stimulated endocytosis (16). We asked whether constitutive Ack1 activation could restore the endocytic brake and thereby rescue the DAT(R615C) gain-of-function endocytic phenotype. DAT(R615C) expressed in SK-N-MC cells internalized significantly faster than wild-type DAT (Fig. 5E and F) and was defective in PKC-stimulated endocytosis (Fig. S3B), consistent with the previous report (16). Remarkably, S445P-Ack1 significantly

decreased DAT(R615C) basal endocytosis to wild-type DAT levels (Fig. 5D), but did not restore PKC-stimulated endocytosis (Fig. S3B).

Discussion

Reuptake inhibitors are used to treat a variety of neuropsychiatric disorders, including depression, obsessive-compulsive disorder, and ADHD (10, 35). These agents are differential selective for SERT, NET, and DAT, and their clinical efficacy varies considerably across the population (10, 12). Transporter-specific cellular regulation has the potential to lead to novel and selective therapeutic approaches that manipulate transporters intrinsically, rather

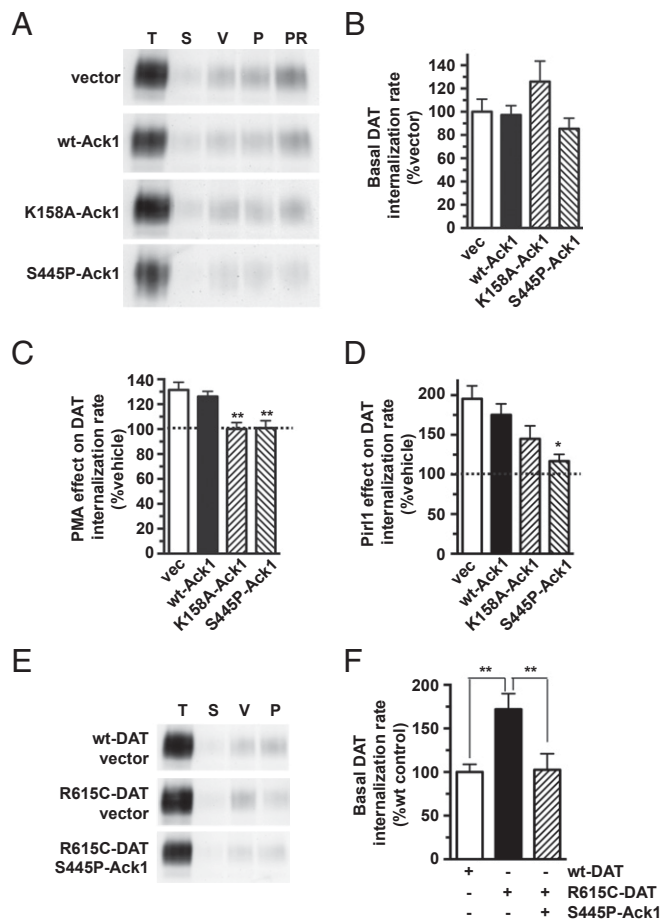


Fig. 5. Ack1 inactivation is required for stimulated DAT endocytosis, and constitutive Ack1 activation rescues ADHD DAT coding variant R615C endocytic dysfunction. Internalization assays: SK-N-MC cells were cotransfected with the indicated DAT and Ack1 isoforms and DAT internalization rates were measured during treatment $\pm 1 \mu\text{M}$ PMA or $20 \mu\text{M}$ pirl1 as described in *SI Methods*. (A–D) Wild-type DAT cotransfected with the indicated Ack1 cDNAs. (A) Representative immunoblots showing total surface DAT at $t = 0$ (T), strip control (S), and internalized DAT during vehicle (V), $1 \mu\text{M}$ PMA (P), or $20 \mu\text{M}$ pirl1 (PR) treatments. (B) Average basal DAT internalization rate expressed as percent vector cotransfected rate \pm SEM, one-way ANOVA; $P = 0.10$; $n = 8$ –9. (C) Average PKC-stimulated DAT internalization rate expressed as percent vector cotransfected rate \pm SEM. $**P < 0.01$ compared with vector control, one-way ANOVA with Dunnett's multiple comparison test; $n = 8$ –9. (D) Average pirl1-stimulated DAT internalization rates expressed as percent vector cotransfected rate \pm SEM. $*P < 0.02$ compared with vector control, one-way ANOVA with Dunnett's multiple comparison test; $n = 8$ –9. (E and F) DAT vs. DAT(R615) internalization rates \pm S445P-Ack1. (E) Representative immunoblots. (F) Average DAT internalization rates expressed as percent wild-type DAT control rate \pm SEM. $**P < 0.01$ compared with indicated sample, one-way ANOVA with Bonferroni's multiple comparison test; $n = 8$ –11.

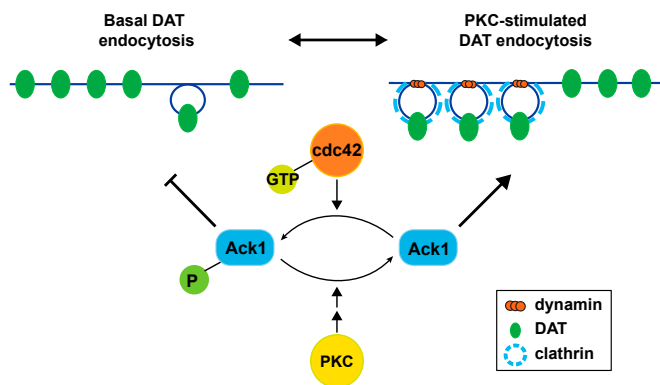


Fig. 6. Model for a PKC-sensitive, Ack1-mediated DAT endocytic brake. Under basal conditions, the cdc42-activated Ack1 pool imposes an endocytic brake upon the plasma membrane DAT population, permitting slow, clathrin- and dynamin-independent DAT endocytosis. PKC activation inactivates Ack1 and releases the DAT endocytic brake, facilitating rapid, clathrin- and dynamin-dependent DAT internalization and intracellular sequestration.

than extrinsically. In the current study, we identified an endocytic regulatory mechanism that is selective for DAT, but not SERT. We previously reported that PKC-stimulated DAT internalization is also selectively dependent upon binding to the neuronal GTPase, Rin, whereas neither SERT nor the GABA transporter binds Rin (36). Taken together with our current findings, these data are consistent with a model wherein distinct mechanisms differentially regulate DAT and SERT surface stability.

There are conflicting reports regarding whether constitutive and regulated DAT internalization are clathrin-dependent. Gene silencing studies suggest that both constitutive and PKC-stimulated DAT internalization in nonneuronal cell lines is clathrin-dependent (37); however, whether chronic clathrin depletion artifactually skews these studies is uncertain. A recent study examining DAT trafficking in a knock-in mouse encoding a DAT extracellular epitope tag observed only modest DAT endocytosis and little/no clathrin colocalization under basal conditions (38). However, it is unclear whether antibody-bound DAT traffics similar to native DAT, as we investigate here. Multiple studies also demonstrate that DAT partitions into cholesterol-rich membrane microdomains (36, 39–44) and that the membrane raft protein flotillin-1 is required for PKC- and AMPH-mediated DAT internalization (42), consistent with a clathrin-independent endocytic mechanism. However, a separate study reported that flotillin-1 contributes to DAT membrane mobility rather than PKC-stimulated DAT internalization (45). Our findings suggest that basal DAT internalization is clathrin-independent, whereas stimulated DAT internalization is clathrin-dependent. Consistent with these data, we previously reported that basal and PKC-stimulated DAT internalization are mediated by independent mechanisms (46, 47) and that constitutive and PKC-stimulated DAT internalization are dynamin-independent and -dependent, respectively (40).

Cdc42 directly activates Ack1, and cdc42 inhibition released the DAT endocytic brake in a manner that required Ack1 inactivation (Fig. 5). Several forms of clathrin-independent endocytosis require cdc42 (48–50). In contrast, we found that cdc42 negatively regulates DAT endocytosis via Ack1 activation (Fig. 3), and that

stimulated DAT endocytosis in response to Ack1 inactivation is clathrin-dependent (Fig. 2). Thus, it appears that cdc42 impacts DAT internalization in a unique fashion, in contrast to its more commonly known function in promoting endocytosis.

Given our current findings, and in light of previous reports, we propose the following model of basal and PKC-regulated DAT endocytosis (Fig. 6). Under basal conditions, an Ack1-mediated endocytic brake stabilizes DAT at the plasma membrane, and cdc42 promotes the braking mechanism via Ack1 activation. Basal internalization that occurs while the endocytic brake is engaged is clathrin- and dynamin-independent. PKC activation decreases Ack1 activity, which releases the endocytic brake and accelerates DAT internalization via a clathrin- and dynamin-dependent mechanism, resulting in intracellular DAT sequestration.

What are the molecular players orchestrating the Ack1-imposed DAT endocytic brake and PKC-mediated Ack1 inactivation? PIP₂ depletion inactivates Ack1 (30), and both DAT (51) and SERT (52) bind to PIP₂. However, DAT mutants lacking PIP₂ binding exhibited plasma membrane instability in HEK cells, whereas disrupting SERT/PIP₂ interactions did not affect SERT membrane trafficking. These findings raise the possibility that PIP₂ effects on Ack1 activity may specifically influence DAT surface stability. PKC activation also increases DAT ubiquitination via a Nedd4-2-mediated mechanism that is required for enhanced DAT endocytosis (53). Nedd4-2 also interacts with Ack1 and is recruited to clathrin-rich vesicles (54), and Nedd4-2/Ack1 interactions drive Ack1 degradation in an Ack1 activity-dependent fashion. Thus, it is possible that Nedd4-2 serves as a dual function player in the DAT endocytic brake by controlling Ack1 protein turnover as well as DAT ubiquitination.

Multiple DAT coding variants and missense mutants have been reported in ADHD, ASD, and infantile Parkinsonism patients, implicating DAT dysfunction as a common risk factor for several DA-related disorders (15–17, 19). Many DAT coding variants exhibit basal anomalous DA efflux and loss of AMPH-induced DA efflux. However, the ADHD-associated DAT(R615C) variant lacks plasma membrane stability due to rapid basal endocytosis and is unable to sequester in response to PKC activation or AMPH exposure. We were able to capitalize on the Ack1-mediated DAT endocytic brake to restore wild-type surface stability to DAT(R615C) (Fig. 5D). Not unexpectedly, S445P-Ack1 also prevented DAT(R615C) from responding to PKC stimulation (Fig. S3B), similar to its effect on wild-type DAT (Fig. 5B). Nevertheless, our ability to rescue DAT(R615C) endocytic dysfunction raises the tantalizing possibility that genetically targeting DAT trafficking may hold promise for DAT coding variants with inherent membrane trafficking dysregulation.

Materials and Methods

All of the methods used in this study have been previously reported by our laboratory. All animal studies were conducted according to University of Massachusetts Medical School Institutional Animal Care and Use Committee-approved protocol A-1506. Transporter function was determined by radio-tracer flux assays (23, 46, 55), and relative initial DAT internalization rates were measured by using reversible biotinylation (23, 36, 40, 47, 56). DAT surface expression changes in cell lines (23, 40, 46, 47, 55, 56) and mouse striatal slices (40, 57) were measured by using surface biotinylation. Finally, DAT surface dynamics were assessed by using TIRFM (40). For detailed experimental protocols, refer to *SI Methods*.

ACKNOWLEDGMENTS. This work was supported by NIH Grant R01DA035224 (to H.E.M.).

- Hyman SE, Malenka RC, Nestler EJ (2006) Neural mechanisms of addiction: The role of reward-related learning and memory. *Annu Rev Neurosci* 29:565–598.
- Iversen SD, Iversen LL (2007) Dopamine: 50 years in perspective. *Trends Neurosci* 30(5):188–193.
- Snyder SH (2002) Forty years of neurotransmitters: A personal account. *Arch Gen Psychiatry* 59(11):983–994.

- Amara SG, Kuhar MJ (1993) Neurotransmitter transporters: Recent progress. *Annu Rev Neurosci* 16:73–93.
- Kristensen AS, et al. (2011) SLC6 neurotransmitter transporters: Structure, function, and regulation. *Pharmacol Rev* 63(3):585–640.
- Bröer S, Gether U (2012) The solute carrier 6 family of transporters. *Br J Pharmacol* 167(2):256–278.

7. Torres GE, Gainetdinov RR, Caron MG (2003) Plasma membrane monoamine transporters: Structure, regulation and function. *Nat Rev Neurosci* 4(1):13–25.
8. Thomsen M, Han DD, Gu HH, Caine SB (2009) Lack of cocaine self-administration in mice expressing a cocaine-insensitive dopamine transporter. *J Pharmacol Exp Ther* 331(1):204–211.
9. Chen R, et al. (2006) Abolished cocaine reward in mice with a cocaine-insensitive dopamine transporter. *Proc Natl Acad Sci USA* 103(24):9333–9338.
10. Iversen L (2006) Neurotransmitter transporters and their impact on the development of psychopharmacology. *Br J Pharmacol* 147(Suppl 1):S82–S88.
11. Gether U, Andersen PH, Larsson OM, Schousboe A (2006) Neurotransmitter transporters: Molecular function of important drug targets. *Trends Pharmacol Sci* 27(7):375–383.
12. Tamminga CA, et al. (2002) Developing novel treatments for mood disorders: Accelerating discovery. *Biol Psychiatry* 52(6):589–609.
13. Jones SR, et al. (1998) Profound neuronal plasticity in response to inactivation of the dopamine transporter. *Proc Natl Acad Sci USA* 95(7):4029–4034.
14. Pinsonneault JK, et al. (2011) Dopamine transporter gene variant affecting expression in human brain is associated with bipolar disorder. *Neuropsychopharmacology* 36(8):1644–1655.
15. Mazei-Robison MS, et al. (2008) Anomalous dopamine release associated with a human dopamine transporter coding variant. *J Neurosci* 28(28):7040–7046.
16. Sakrikar D, et al. (2012) Attention deficit/hyperactivity disorder-derived coding variation in the dopamine transporter disrupts microdomain targeting and trafficking regulation. *J Neurosci* 32(16):5385–5397.
17. Hamilton PJ, et al.; NIH ARRA Autism Sequencing Consortium (2013) De novo mutation in the dopamine transporter gene associates dopamine dysfunction with autism spectrum disorder. *Mol Psychiatry* 18(12):1315–1323.
18. Bowton E, et al. (2014) SLC6A3 coding variant Ala559Val found in two autism probands alters dopamine transporter function and trafficking. *Transl Psychiatry* 4:e464.
19. Hansen FH, et al. (2014) Missense dopamine transporter mutations associate with adult parkinsonism and ADHD. *J Clin Invest* 124(7):3107–3120.
20. Mergy MA, et al. (2014) The rare DAT coding variant Val559 perturbs DA neuron function, changes behavior, and alters in vivo responses to psychostimulants. *Proc Natl Acad Sci USA* 111(44):E4779–E4788.
21. Melikian HE (2004) Neurotransmitter transporter trafficking: Endocytosis, recycling, and regulation. *Pharmacol Ther* 104(1):25–42.
22. Rudnick G, Krämer R, Blakely RD, Murphy DL, Verrey F (2014) The SLC6 transporters: Perspectives on structure, functions, regulation, and models for transporter dysfunction. *Pflugers Arch* 466(1):25–42.
23. Boudanova E, Navaroli DM, Stevens Z, Melikian HE (2008) Dopamine transporter endocytic determinants: Carboxy terminal residues critical for basal and PKC-stimulated internalization. *Mol Cell Neurosci* 39(2):211–217.
24. Sorkina T, Richards TL, Rao A, Zahniser NR, Sorkin A (2009) Negative regulation of dopamine transporter endocytosis by membrane-proximal N-terminal residues. *J Neurosci* 29(5):1361–1374.
25. Galisteo ML, Yang Y, Ureña J, Schlessinger J (2006) Activation of the nonreceptor protein tyrosine kinase Ack by multiple extracellular stimuli. *Proc Natl Acad Sci USA* 103(26):9796–9801.
26. Linseman DA, Heidenreich KA, Fisher SK (2001) Stimulation of M3 muscarinic receptors induces phosphorylation of the Cdc42 effector activated Cdc42Hs-associated kinase-1 via a Fyn tyrosine kinase signaling pathway. *J Biol Chem* 276(8):5622–5628.
27. Teo M, Tan L, Lim L, Manser E (2001) The tyrosine kinase ACK1 associates with clathrin-coated vesicles through a binding motif shared by arrestin and other adaptors. *J Biol Chem* 276(21):18392–18398.
28. Yang W, Lo CG, Dispenza T, Cerione RA (2001) The Cdc42 target ACK2 directly interacts with clathrin and influences clathrin assembly. *J Biol Chem* 276(20):17468–17473.
29. Ureña JM, et al. (2005) Expression, synaptic localization, and developmental regulation of Ack1/Pyk1, a cytoplasmic tyrosine kinase highly expressed in the developing and adult brain. *J Comp Neurol* 490(2):119–132.
30. Shen H, et al. (2011) Constitutive activated Cdc42-associated kinase (Ack) phosphorylation at arrested endocytic clathrin-coated pits of cells that lack dynamin. *Mol Biol Cell* 22(4):493–502.
31. Yokoyama N, Miller WT (2003) Biochemical properties of the Cdc42-associated tyrosine kinase ACK1. Substrate specificity, autophosphorylation, and interaction with Hck. *J Biol Chem* 278(48):47713–47723.
32. Mahajan K, et al. (2010) Effect of Ack1 tyrosine kinase inhibitor on ligand-independent androgen receptor activity. *Prostate* 70(12):1274–1285.
33. Lin Q, Wang J, Childress C, Yang W (2012) The activation mechanism of ACK1 (activated Cdc42-associated tyrosine kinase 1). *Biochem J* 445(2):255–264.
34. Mahajan NP, Whang YE, Mohler JL, Earp HS (2005) Activated tyrosine kinase Ack1 promotes prostate tumorigenesis: Role of Ack1 in polyubiquitination of tumor suppressor Wwox. *Cancer Res* 65(22):10514–10523.
35. Iversen L (2000) Neurotransmitter transporters: Fruitful targets for CNS drug discovery. *Mol Psychiatry* 5(4):357–362.
36. Navaroli DM, et al. (2011) The plasma membrane-associated GTPase Rin interacts with the dopamine transporter and is required for protein kinase C-regulated dopamine transporter trafficking. *J Neurosci* 31(39):13758–13770.
37. Sorkina T, Hoover BR, Zahniser NR, Sorkin A (2005) Constitutive and protein kinase C-induced internalization of the dopamine transporter is mediated by a clathrin-dependent mechanism. *Traffic* 6(2):157–170.
38. Block ER, et al. (2015) Brain region-specific trafficking of the dopamine transporter. *J Neurosci* 35(37):12845–12858.
39. Kovtun O, et al. (2015) Single-quantum-dot tracking reveals altered membrane dynamics of an attention-deficit/hyperactivity-disorder-derived dopamine transporter coding variant. *ACS Chem Neurosci* 6(4):526–534.
40. Gabriel LR, et al. (2013) Dopamine transporter endocytic trafficking in striatal dopaminergic neurons: Differential dependence on dynamin and the actin cytoskeleton. *J Neurosci* 33(45):17836–17846.
41. Jones KT, Zhen J, Reith ME (2012) Importance of cholesterol in dopamine transporter function. *J Neurochem* 123(5):700–715.
42. Cremona ML, et al. (2011) Flotillin-1 is essential for PKC-triggered endocytosis and membrane microdomain localization of DAT. *Nat Neurosci* 14(4):469–477.
43. Foster JD, Adkins SD, Lever JR, Vaughan RA (2008) Phorbol ester induced trafficking-independent regulation and enhanced phosphorylation of the dopamine transporter associated with membrane rafts and cholesterol. *J Neurochem* 105(5):1683–1699.
44. Adkins EM, et al. (2007) Membrane mobility and microdomain association of the dopamine transporter studied with fluorescence correlation spectroscopy and fluorescence recovery after photobleaching. *Biochemistry* 46(37):10484–10497.
45. Sorkina T, Caltagaroni J, Sorkin A (2013) Flotillins regulate membrane mobility of the dopamine transporter but are not required for its protein kinase C dependent endocytosis. *Traffic* 14(6):709–724.
46. Holton KL, Loder MK, Melikian HE (2005) Nonclassical, distinct endocytic signals dictate constitutive and PKC-regulated neurotransmitter transporter internalization. *Nat Neurosci* 8(7):881–888.
47. Loder MK, Melikian HE (2003) The dopamine transporter constitutively internalizes and recycles in a protein kinase C-regulated manner in stably transfected PC12 cell lines. *J Biol Chem* 278(24):22168–22174.
48. Sabharanjak S, Sharma P, Parton RG, Mayor S (2002) GPI-anchored proteins are delivered to recycling endosomes via a distinct cdc42-regulated, clathrin-independent pinocytotic pathway. *Dev Cell* 2(4):411–423.
49. Massol P, Montcourrier P, Guillemot JC, Chavrier P (1998) Fc receptor-mediated phagocytosis requires CDC42 and Rac1. *EMBO J* 17(21):6219–6229.
50. Gauthier NC, et al. (2005) Helicobacter pylori VacA cytotoxin: A probe for a clathrin-independent and Cdc42-dependent pinocytotic pathway routed to late endosomes. *Mol Biol Cell* 16(10):4852–4866.
51. Hamilton PJ, et al. (2014) PIP2 regulates psychostimulant behaviors through its interaction with a membrane protein. *Nat Chem Biol* 10(7):582–589.
52. Buchmayer F, et al. (2013) Amphetamine actions at the serotonin transporter rely on the availability of phosphatidylinositol-4,5-bisphosphate. *Proc Natl Acad Sci USA* 110(28):11642–11647.
53. Vina-Vilaseca A, Sorkin A (2010) Lysine 63-linked polyubiquitination of the dopamine transporter requires WW3 and WW4 domains of Nedd4-2 and UBE2D ubiquitin-conjugating enzymes. *J Biol Chem* 285(10):7645–7656.
54. Chan W, et al. (2009) Down-regulation of active ACK1 is mediated by association with the E3 ubiquitin ligase Nedd4-2. *J Biol Chem* 284(12):8185–8194.
55. Melikian HE, Buckley KM (1999) Membrane trafficking regulates the activity of the human dopamine transporter. *J Neurosci* 19(18):7699–7710.
56. Boudanova E, Navaroli DM, Melikian HE (2008) Amphetamine-induced decreases in dopamine transporter surface expression are protein kinase C-independent. *Neuropharmacology* 54(3):605–612.
57. Gabriel LR, Wu S, Melikian HE (2014) Brain slice biotinylation: An ex vivo approach to measure region-specific plasma membrane protein trafficking in adult neurons. *J Vis Exp* 86(86):51240.